PASJ: Publ. Astron. Soc. Japan , 1–??, ⟨publication date⟩

Broad-Band Spectrum of The Black Hole Candidate IGR J17497–2821 Studied with *Suzaku*

Adamantia Paizis[1,2], Ken Ebisawa[2], Hiromitsu Takahashi[3], Tadayasu Dotani[2], Takayoshi Kohmura[4], Motohide Kokubun[2], Jérôme Rodriguez[5], Yoshihiro Ueda[6], Roland Walter[7], Shin'ya Yamada[8], Kazutaka Yamaoka[9], Takayuki Yuasa[8]

[1]*Istituto Nazionale di Astrofisica, IASF*
Via Bassini 15, 20133 Milano, Italy
[2]*Institute of Space and Astronautical Science, JAXA*
3–1–1, Yoshinodai, Sagamihara, Kanagawa, 229-8510, Japan
[3]*Department of Physical Science, School of Science, Hiroshima University*
1-3-1 Kagamiyama, Higashi-Hiroshima, Hiroshima 739-8526, Japan
[4]*Department of Physics, Kogakuin University*
2665-1, Nakano-cho, Hachioji, Tokyo, 192-0015, Japan
[5]*CEA Saclay, DSM/DAPNIA/Service d'Astrophysique*
FR-91 191 Gif-sur-Yvette Cedex, France
[6]*Department of Astronomy, Kyoto University*
Kitashirakawa-Oiwake-cho, Sakyo-ku, Kyoto, 606-8502, Japan
[7]*INTEGRAL Science Data Centre*
Chemin d'Ecogia 16, 1290 Versoix, Switzerland
[8]*Department of Physics, University of Tokyo*
7-3-1, Hongo, Bunkyo-ku, Tokyo, 113-0033, Japan
[9]*Department of Physics, Aoyama Gakuin University*
5-10-1 Fuchinobe, Sagamihara, Kanagawa 229-8558, Japan
ada@iasf-milano.inaf.it

(Received ⟨2008 July 15⟩; accepted ⟨2008 October 12 ⟩)

Abstract

The broad-band 1–300 keV *Suzaku* spectrum of IGR J17497–2821, the X-ray transient discovered by *INTEGRAL* in September 2006, is presented. *Suzaku* observed IGR J17497–2821 on September 25, eight days after its discovery, for a net exposure of about 53 ksec. During the *Suzaku* observation, IGR J17497–2821 is very bright, 2×10^{37} erg s^{-1} at 8 kpc in the 1–300 keV range, and shows a hard spectrum, typical of black hole candidates in the low-hard state. Despite the multi-mission X-ray monitoring of the source, only with *Suzaku* is it possible to obtain a broad-band spectrum in the 1–300 keV range with a very high signal to noise ratio. A sum of a multi-color disc (DISKBB) and a thermal Comptonization component (COMPPS) with mild reflection is a good representation of our IGR J17497–2821 *Suzaku* spectrum. The spectral properties of the accretion disc as well as the cut-off energy in the spectrum at about 150 keV are clearly detected and constrained. We discuss the implications on the physical model used to interpret the data and the comparison with previous results.

Key words: accretion disks — black hole physics — stars: individual (IGR J17497–2821)— X-ray: binaries

1. Introduction

On 2006 September 17 a new hard X-ray transient, IGR J17497–2821 (Soldi et al. 2006), was discovered by *INTEGRAL* (Winkler et al. 2003). In the quest to understand the nature of this new transient, many follow-up observations were performed. Neither X-ray bursts nor pulsations, that would point to the presence of a neutron star, were found in *RXTE* data (Rodriguez et al. 2007). *INTEGRAL-Swift* (Walter et al. 2007) and *RXTE* (Rodriguez et al. 2007) studies showed that the source had a very hard spectrum being detected up to about 200 keV. A phenomenological description of the *INTEGRAL-Swift* data led to an absorbed cut-off power-law with photon spectral index $\Gamma\sim1.7$ and cut-off around 200 keV (Walter et al. 2007). The spectrum was also fitted with the thermal Comptonization model COMPTT (Titarchuk 1994) obtaining a plasma temperature of about 35 keV. As the authors point out, this temperature is coupled to the optical depth of the plasma and the resulting temperature was poorly constrained: $kT_e=35^{-9}_{+200}$ keV.
Also Rodriguez et al., (2007) fit the data with COMPTT but, as they also point out, the parameters inferred were limited by the energy range studied (3–180 keV): the seed photon temperature was frozen to 0.1 keV and a Comptonizing plasma temperature of about 35 keV and

optical depth $\tau \sim 2$ was obtained. Two weeks after the source discovery, a *Chandra* observation was performed (Paizis et al. 2007). The narrow *Chandra* energy range was not sensitive to the high energy cut-off and the spectrum could be fit with an absorbed power-law with a slope of about 1.2.

Optical, near infra-red (NIR) and radio counterparts were searched for thanks to the *Chandra* 0.6 arcsec positional accuracy. The NIR counterpart was identified with a red giant K-type companion (Paizis et al. 2007; Torres et al. 2006). The NIR variability of the source (Torres et al. 2007; Walter et al. 2007) confirmed the association and was consistent with a late-type companion located close to the Galactic center. Only an upper limit could be found for the optical band (V>23), as expected for a source placed near or beyond the Galactic centre. No radio counterpart was found down to a limit of 0.21 mJy at 4.80 and 8.64 GHz (Rodriguez et al. 2007). Consistently with previous studies, we assume an 8 kpc distance to the source. As can be seen, IGR J17497–2821 has been throughly observed during its outburst decay and the information gathered from various X-ray, radio and NIR observations, points to the source being an X-ray Nova, a Low Mass X-ray Binary (LMXB) hosting a black hole (BH).

About eight days after the source discovery, *Suzaku* observed IGR J17497–2821 with a net exposure of about 53 ksec. IGR J17497–2821 was at 80% of its peak flux, about 80 mCrab in the 15–50 keV band. Preliminary results were presented by Itoh et al. (2006) and showed that the source could be detected up to ∼300 keV. In this work we analyze in detail the *Suzaku* observation of IGR J17497–2821.

2. Observation and Data Analysis

Suzaku (Mitsuda et al. 2007) observed IGR J17497–2821 about eight days after its discovery, starting from 2006 September 25, 07:00 UT, up to September 26, 14:14 UT, for a total of about 53 ksecs. The data were acquired with the X-ray Imaging Spectrometer (XIS, 0.12-12 keV: Koyama et al. 2007) and the Hard X-ray Detector (HXD, 10–600 keV: Takahashi et al 2007; Kokubun et al. 2007). The XIS detectors are located at the aim-points of the XRT mirrors (Serlemitsos et al. 2007). The viewing of the current observation is HXD-nominal.

2.1. XIS Data Selection and Processing

Given the brightness of IGR J17497–2821, XIS was mainly operated with the Burst and Window (1/4) options, with only a few tens of seconds of data taken in the Normal mode (ignored in this work). These options, more suitable for bright sources in order to minimize pile-up, prevented us from carrying on power spectra analysis since about 50% of the 2 sec GTIs are data-free.

Out of the four XIS, the three front-illuminated ones (FI, XIS 0 2 3) were mostly used in the 2x2 editing mode with only a small fraction of data taken in the 3x3 mode, while the fourth XIS (the back-illuminated, BI CCD, XIS 1) was operated only in 3x3 editing mode. During the observation a dark frame/light leak error occurred in the sensors almost simultaneously, the error being restricted to RAWY<118. The inclusion of these data resulted in an apparent flux decrease in all XIS sensors hence in all the analysis the data from the segments with RAWY<256 were not used. This selection results in a ∼25% reduction in the XIS normalization constant. Partial telemetry saturation occurring in one of the four segments reduces a few percent more the XIS normalization. Apart from the dark frame correction, the data were analyzed in the standard way.

2.2. HXD Data Selection and Processing

The HXD was operated in the normal mode and we performed the analysis in the standard way described in the *Suzaku* data reduction documentation[1]. Unlike XIS, HXD is not an imaging instrument and it is not possible to obtain background data from the observation data themselves. Hence the HXD team has developed a model of the time-variable particle background (Non X-ray Background, NXB). HXD NXB and response files were downloaded from the instrument team web pages [2], together with the GSO additional ancillary file distributed by the instrument team to match the Crab spectrum in the GSO energy range[3]. Given the source brightness, the cosmic X-ray background spectrum was not included in the HXD analysis (less than 0.6% of the observed rate).

A limiting factor for the sensitivity of the HXD-GSO is the reproducibility in the background estimation (systematic error), rather than the statistical error. In order to accurately assess the systematic error specific to our observation, we compared the nominal NXB spectrum (the model) with the spectrum obtained during earth occultation, as done in Fukazawa et al. 2008. The earth occultation "total-background" spectrum is shown in black in Fig. 1. In the ideal case (model=real background) we would expect the subtracted spectrum to be equal to zero, whereas in the plot it is slightly over zero and close to the red spectrum (1% of the background spectrum). This means that during the earth occultation time of our observation, and presumably also during the nearby source observation time, the NXB model spectrum is underestimated and is most likely about 1% higher. In our analysis we have applied a 1.2% increase in the background spectrum that corresponds to a 2σ deviation in the all-data distribution of Fukazawa et al. 2008.

We note that while the HXD field of view below 100 keV is very small, $34' \times 34'$, minimizing source contamination issues, the field of view above 100 keV is of $4.5^\circ \times 4.5^\circ$, hence contamination could be occurring. During the IGR J17497–2821 outburst, *INTEGRAL* detected only two sources above 100 keV: IGR J17497–2821 and 1E 1740.7–2942 (the "great annihilator"), 2° away (Walter et al. 2007), with IGR J17497–2821 clearly out-

[1] http://www.astro.isas.ac.jp/suzaku/analysis/

[2] PIN: http://www.astro.isas.ac.jp/suzaku/analysis/hxd/pinnxb/
GSO: http://www.astro.isas.ac.jp/suzaku/analysis/hxd/gsonxb/

[3] http://www.astro.isas.ac.jp/suzaku/analysis/hxd/gsoarf/

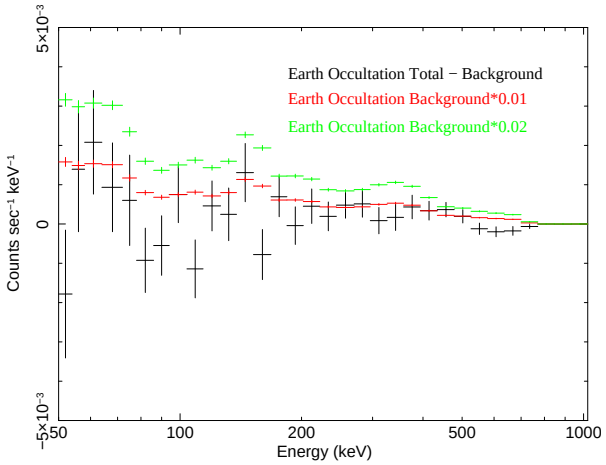

Fig. 1. Earth occultation total-background spectrum (black) used to compare between the data and the model prediction. The 1% (red) and 2% (green) levels of the background are also shown.

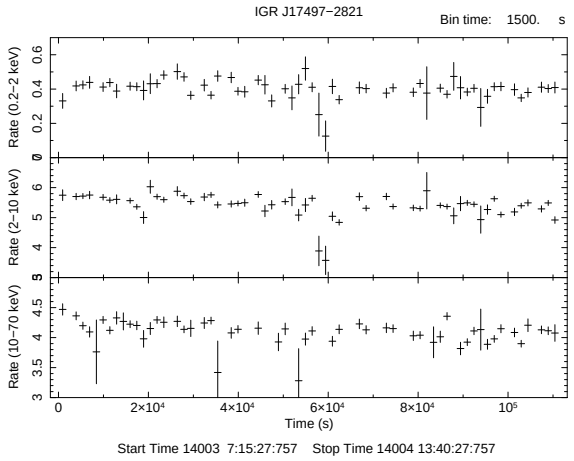

Fig. 2. BI-XIS and PIN background subtracted IGR J17497–2821 lightcurves with a 1500 sec time bin are shown. From top, the three panels refer to soft XIS band (0.2–2 keV), hard XIS (2–10 keV) and PIN (10–70 keV).

shining the "great annihilator" at its outburst peak. The *Suzaku* observation occurred when IGR J17497–2821 was still at 80% of its peak flux and very little contamination is expected to occur between 100–160 keV where the transmission rate of the collimator is as low as 10% for a 2° off axis source in the HXD field. No contamination is expected above 160 keV where IGR J17497–2821 is the only active source, see Fig. 1 in Walter et al., 2007.

2.3. Spectral fitting

Spectral fitting was performed with the XSPEC v12 software package. The XIS source spectra obtained with the two different editing modes (2x2 and 3x3) in XIS 0 2 3 have been co-added in a final "XIS-FI-spectrum", whereas the "XIS-BI-spectrum" has been kept separate due to the differences in the response matrix. In the spectral fitting the 1–8 keV XIS range was used, allowing for an energy offset within ±17 eV, to account for the current uncertainty in the XIS energy scale (Makishima et al. 2008). The gain of the two XIS spectra was also left free and always resulted to be close to 1 (1% deviation in the worst case). As for HXD, spectral fitting was carried on in the 12–70 keV and 70–300 keV band for PIN and GSO, respectively.

The overall model normalizations were allowed to differ between the XIS-FI, XIS-BI and HXD spectra but were constrained to be the same between HXD-PIN and HXD-GSO that we fixed to 1.13. No systematic error was added to the XIS data.

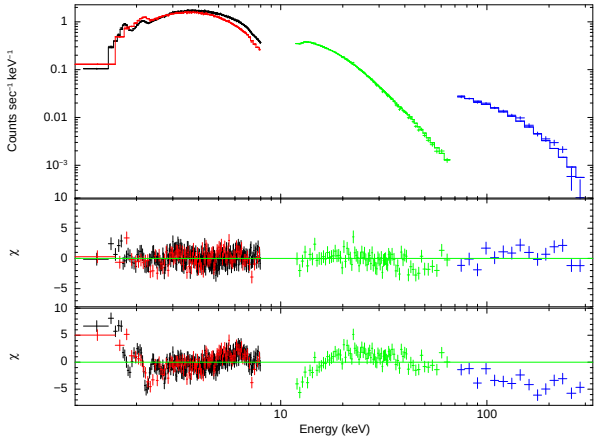

Fig. 3. *Upper panel* Background subtracted time-averaged XIS-FI (black), XIS-BI (red), HXD-PIN (green) and HXD-GSO (dark blue) spectra of IGR J17497–2821. The *intermediate panel* shows the residuals using the best fit WABS*EDGE*CUTOFFPL model given in Tab 1 while the lower panel shows the single WABS*PL fit model. See text.

3. Results

In this section we describe the results we obtain from the *Suzaku* data analysis both in terms of phenomenological and physical models. In the end, we include our results in the frame of a wider spectral evolution study of the IGR J17497–2821 outburst, treating in a consistent way all the currently available high energy spectra of the source.

3.1. Suzaku results: from phenomenology to physics

In Fig. 2 the XIS (soft and hard X-ray band) and HXD-PIN count rate evolution of IGR J17497–2821 is given (1500 sec time bin). The overall XIS 2–10 keV plot shows a slow but constant rate decrease along our observation. A similar behaviour occurs also in the PIN 10–70 keV showing that the source did not switch between different spectral states. The XIS to PIN rate hardness ratio is quite constant hence we add all the available data to obtain one time-averaged spectrum per instrument. This is a good representation of the source spectral behaviour and furthermore increases the statistics of the spectra, essential for the high energy cut-off investigation.

To have the feeling of the shape of the spectrum, we first decided to find the appropriate phenomenological model to fit the data starting from the simplest case,

Table 1. Best-fit model: WABS*EDGE*CUTOFFPL[†,‡].

N_H (10^{22} cm^{-2})	Γ	E_{cut} (keV)	E_{edge} (keV)	Tau_{edge}
4.56±0.02	$1.45^{+0.02}_{-0.01}$	150^{+7}_{-4}	[7.11]	[0.05]
χ^2_ν(dof)=1.085 (1158)				

† Errors are computed at 90% confidence level for a single parameter.
‡ The parameters of the EDGE component were frozen to the best fit values obtained from the XIS fit alone.

a single absorbed power-law (WABS*PL, with absorption model by Morrison and McCammon 1983). This model is clearly not a good representation of the data as can be seen in Fig. 3, *lower panel*. Hence we preceeded with an absorbed power-law with an exponential roll-over (CUTOFFPL). The fit improved significantly, confirming that the overall IGR J17497–2821 spectrum (Γ∼1.45) indeed breaks above 80 keV. Fig. 3 *medium and upper panel* show the best fit obtained including also an absorption edge (EDGE), needed in the XIS data when investigated separately from HXD (probability of $\sim10^{-5}$ that the improvement was purely due to chance). In the fit using only XIS data, the (fixed) 7.11 keV Fe edge shows an optical depth of 0.05±0.02. Hereafter in the complete XIS-HXD fits performed, we freeze the value of the 2 parameters describing the absorption edge to what obtained from the XIS spectra alone. Details of the final best fit model are given in Table 1. A background deviation from the 1.2% case used here (Section 2.2) does not affect the power-law slope value that is mainly driven by the XIS+PIN spectral shape. Indeed a Γ=1.45±0.01 is obtained for the nominal, 0% increase, NXB.

A cut-off power-law shape suggests that the spectrum can be described in terms of a thermal Comptonization model. Among all the available models we choose COMPPS (Poutanen & Svensson 1996). The high energy cut-off found from the phenomenological fit implies a hot Comptonizing corona for which COMPPS (unlike e.g. COMPTT) is suitable. Fitting the IGR J17497–2821 spectrum with an absorbed EDGE*COMPPS component did not result in a good fit as can be seen in Fig. 4, *lower residual panel*. A clear soft excess is visible in the low end of XIS data as well as a clear "S" shape in the HXD domain (χ^2_ν=1.3, 1157 dof). As a first improvement we add a soft component to account for the excess. A natural candidate is a cold disc emission and we choose the DISKBB representation of it (Mitsuda et al. 1984). The seed photon temperature of the two models (DISKBB and COMPPS) were constrained to a single value and the model used is an absorbed EDGE*(COMPPS+DISKBB). Fig. 4, *intermediate residual panel*, shows that although the soft excess description improved, the HXD part of the spectrum is still not correctly described ("S" shape in the residuals, $\chi^2_\nu\sim$1.2, 1156 dof).
The residuals of the high energy detector, "S" shape, resemble what obtained by Makishima et al. 2008 and Takahashi et al. 2008 in the study of two other BH binaries, Cyg X–1 and GRS J1655–40, respectively. Similarly to these authors, we included the reflection option in the COMPPS model, letting free the REL_REFL parameter that indicates the solid angle of the cold material visible from the Comptonizing source, in units of 2π. Since the reflection component includes also the absorption edge, we did not include it explicitely in the model. Furthermore, in the spectral fitting, we included a 6.4 keV Fe line, expected in the presence of reflection from a cold disk. In the broad band fit, the line width was frozen to the best fit value obtained by the spectral fitting of XIS data alone, 0.39 keV. With a reflection of about 0.17 the fit improved significantly ($\chi^2_\nu\sim$1.07, 1154 dof) as shown in Fig. 4, *upper residual panel and fit*. Details of this best fit model are shown in Table 2 while the unabsorbed best fit model is shown in Fig. 5.
In the COMPPS model we have assumed a spherically symmetric corona (GEOM=4, see Table 2) where the seed photons are injected in the center of the sphere. Under such a configuration, the energy spectrum of the Compton upscattered emission has no dependence on the source inclination angle, that we assumed to be i=60°.
We note that unlike the case of Makishima et al. 2008 and Takahashi et al. 2008 a two component COMPPS model besides DISKBB is not needed. While in their case this interpretation was supported by the fact that the two different Comptonizing regions indeed showed different optical depth (ratio of a few), in our case this is not true and a double COMPPS model still returns a single Comptonizing region. The reason for this could be the high absorption we detect in the spectrum of IGR J17497–2821 with respect to GRO J1655–40 and Cyg X–1 (an order of magnitude higher). This, combined to the worse statistics, hampers the detection of the second "soft" COMPPS that dominated below ∼3 keV (compare our unabsorbed best fit model shown in Fig. 5, with Fig. 5 in Makishima et al. 2008).
We believe that the model given in Table 2 is the best physical representation we can extract from the current data, χ^2_ν is acceptable and there is no clear feature in the obtained residuals that would require a physics-driven additional component.

3.2. Long-term spectral variability

IGR J17497–2821 has been observed by more than one high energy mission along its decay. Different missions introduce instrumental differences, furthermore it is not always possible to compare the results published by the authors due to different models used. To overcome the bias introduced from different models, we decided to fit all the published spectra in terms of the same model, to ease the comparison[4]. We choose the model of Table 1: WABS*EDGE*CUTOFFPL. In all cases the values of N_H and the EDGE were frozen to the values of Table 1, to avoid the bias they introduce in the power-law photon index. Only three parameters, Γ, E_{cut} and normalization, were let free. *RXTE* data, presented in Rodriguez et al. 2007, span from September 20 up to September 29, 2006. During

[4] Co-authors of this paper have been the leading authors of the multi-mission follow-up.

Table 2. Best-fit model:WABS*(GAUSS+DISKBB+COMPPS)[§,†,§§]

N_H ($\times10^{22}$ cm^{-2})	kT_{in}^{diskbb} (keV)	r_{in}^{diskbb} (km)	kT_{in}^{compps} (keV)	r_{in}^{compps} (km)	kT_e (keV)	τ	Refl.	EW_{line}[¶] (eV)
$5.15^{+0.01}_{-0.03}$	$0.25^{+0.01}_{-0.02}$	123^{+33}_{-4}	=DISKBB	53^{+2}_{-4}[‡]	85±9	$1.42^{+0.25}_{-0.15}$	0.17±0.03	37±10

χ^2_ν(dof)=1.07 (1154)

§ Errors are computed at 90% confidence level for a single parameter.
† IGR J17497–2821 is assumed to be at a distance of 8 kpc with an inclination i=60°.
§§ A spherical corona configuration is assumed i.e. GEOM=4.
‡ Not corrected for the inclination, see text.
¶ The center and width of the line were fixed at 6.4 keV and 0.39 keV respectively, as obtained by the XIS data alone. See text.

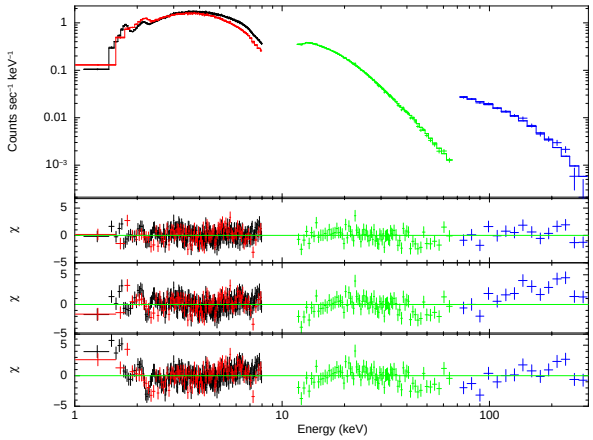

Fig. 4. As in Fig. 3 but with WABS*EDGE*COMPPS (residuals in the lower panel), WABS*EDGE*(DISKBB+COMPPS) (residuals in the middle panel), and WABS*(GAUSS+DISKBB+COMPPS) with reflection (residuals in the upper panel and fit, Table 2).

all the *RXTE* follow-up, IGR J17497–2821 remained constant with $\Gamma\sim1.55$. *INTEGRAL-Swift* (Walter et al. 2007) and *Suzaku* spectra (this work) were taken during the period covered by *RXTE* (20-22 September the former and 25-26 September the latter). Our fit returns a power-law slope Γ=1.67±0.05 for the former case (*INTEGRAL-Swift*), and $\Gamma=1.45^{+0.02}_{-0.01}$ in the latter (*Suzaku*, Table 1). Most likely this slope difference is due to instrumental cross-calibration effects since it occurs during the period when the source was seen to be constant by *RXTE*. The *Chandra*/HETGS spectrum (Paizis et al. 2007) that refers to a later observation, October 1, returns a slope of Γ=1.17±0.02, considerably harder than what previously obtained. In this case we have frozen E_{cut} to the *Suzaku* value, 150 keV, being the cut-off considerably beyond the *Chandra* energy range. The source is rather constant during the *Chandra* observation and instrumental issues, at the origin of the hard spectrum, such as a high pile-up are very unlikely since the pile-up fraction in the HETGS arms is about 2% (Paizis et al. 2007). A possible reason for the hard spectrum obtained in *Chandra* data could be the heavy absorption of the system that leaves a *Chandra* effective energy range that is very narrow (1.5-8 keV), possibly introducing a bias in the result. To test this hypothesis, we fit the *Suzaku*/XIS data alone so that we "reproduce" the *Chandra* energy range. Fixing N_H, EDGE parameters and E_{cut} to what found in Table 1, we find that the XIS spectrum is still consistent with the broad band result, Γ=1.45± 0.01 (χ^2_ν=1.042, 1064 dof) hence the *Chandra* spectrum is indeed hard. This suggests that IGR J17497–2821 remained roughly constant for about 9 days (*RXTE* period) to suddenly harden two days later. Another possibility is that a change of hydrogen column density occurred in the system causing the apparent change of slope. Indeed IGR J17497–2821 appears to have a significant contribution from the local matter near the binary system, its hydrogen column density $N_H=(4–5)\times10^{22}$ cm^{-2} is in fact larger that the galactic one $\sim1.5\times10^{22}$ cm^{-2} (Dickey & Lockman 1990). Nevertheless, the spectral change cannot be ascribed to a variability of N_H alone since the *Chandra* spectrum is not compatible with a fixed *Suzaku* value of Γ=1.45, no matter what the value of N_H (χ^2_ν=1.32 for 336 dof and probability of $\sim10^{-13}$ that the improvement was purely due to chance from a frozen Γ=[1.45] to a free $\Gamma\sim1.2$). Hence, most likely, a combination of an increase in N_H and spectral hardening occurred along the outburst.
We note that the attempt to explain the spectral hardening in terms of the disappearing disk (DISKBB) alone does not work since the *Suzaku* data require the *shape* of the spectrum to be changed and not the normalizations of the two components alone.
Fig 6 shows the two extremes: the *INTEGRAL-Swift* peak best fit model, together with the *Chandra*/HETG spectra. In about nine days (from peak flux to *Chandra* follow-up), the 2–10 keV flux of IGR J17497–2821 decreased by about 50% whereas the 15–50 keV flux decreased by about 20% only (Paizis et al. 2007), i.e. the source seems to have started hardening about nine days after the peak.

Besides *Suzaku*, only the *Chandra* observation of IGR J17497–2821 (Paizis et al. 2007), did show evidence of an accretion disc ($kT_{in}\sim0.2$ keV) and it would be interesting to compare the temperature and radius of the disc in the two cases. Unfortunately the overall spectral

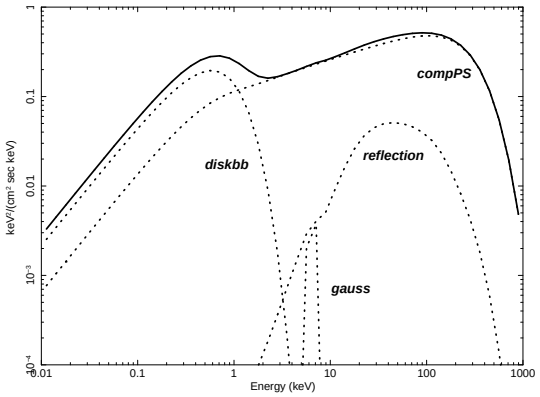

Fig. 5. Unabsorbed best fit model used to fit the IGR J17497–2821 *Suzaku* spectrum, GAUSS+DISKBB+COMPPS in Table 2..

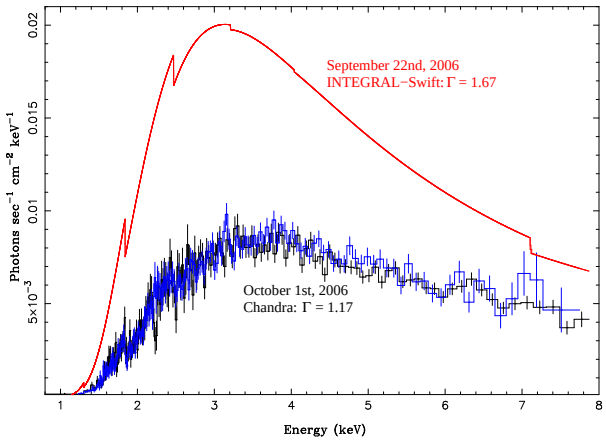

Fig. 6. Best fit model of the outburst peak compared to the Chandra follow-up data. Axes have been left linear to better visualize the slope differences.

shape is different in the two cases and in the soft part of the spectrum, where N_H, DISKBB and soft end of the PL co-exist, it is not possible to disentangle the different contributions to isolate the disc variability.

4. Discussion

We have presented the broad band X-ray spectrum of IGR J17497–2821 obtained with *Suzaku* eight days after the discovery and investigated the long-term spectral variability in the two weeks following the source discovery. During the *Suzaku* observation, the source unabsorbed flux in the 1–300 keV band is about 3×10^{-9} erg s^{-1} cm^{-2} that, for an assumed distance of 8 kpc, leads to a luminosity of about 2×10^{37} erg s^{-1}.

4.1. Suzaku broad-band spectrum and implications

The high signal to noise ratio achieved in the soft end of the *Suzaku* spectrum, together with the low energy threshold, allowed us to constrain the parameters that describe the thermal part of the spectrum. Unlike what obtained with *INTEGRAL* and *RXTE*, the soft component, interpreted as the accretion disk, is well constrained, see Table 2. This is also the case for the reflection component detected for the first time in IGR J17497–2821. The DISKBB component has a raw innermost radius r_{in}∼123 km (assumed 8 kpc distance and 60° inclination) which yields to the best-estimate actual inner radius R_{in}∼145 km, obtained applying nominal correction factors in Makishima et al. 2000, including the color hardening factor of 1.7. Conversely, the COMPPS component has an innermost radius r_{in}^{seed}∼53 km that leads to a corrected inner radius R_{in}^{seed}∼62 km[5]. These two inner radii provide an indication of the size of the emitting areas and in our case the region directly visible is about $(123/53)^2 = 5.4$ times larger than the seed photon region (i.e. ∼84% of photons are directly visible and 16% are covered by the Compton cloud). This may suggest that the Comptonizing plasma has a patchy structure, as suggested also by Gierlinski et al. 1997 and more recently by Makishima et al. 2000 in the case of Cyg X–1.

In order to calculate the best estimate of the inner radius of the (optically thick) disk, we need to measure its total flux. In our case, the normalization of the DISKBB model alone represents only a part of the disc flux since a fraction is Compton up-scattered by the corona and is not observed directly. Hence to obtain the total disc flux it is necessary to combine the information from the DISKBB and COMPPS models, adding quadratically the two obtained inner radii, as done in e.g. Makishima et al. 2008. We obtain a disc inner radius of 158 km, $\sim 11 R_g$ for a 10 solar mass BH. This estimated value for the inner disc radius may be relatively small compared to the idea of disc truncation in the LHS, but it should not be used to rule it out. Indeed, strong conclusions on the real inner disc radius cannot be driven since the results are subject to uncertainties such as the source inclination and distance assumed, the color hardening factor in the LHS, and the validity of the multicolor optically thick description of the disc at all radii (see Makishima et al. 2008 for a detailed discussion).

At the higher end of the spectrum, the cut-off energy we obtain is well below the upper energy boundary of the data, hence we are sampling both the rise and the descent of the spectrum.

IGR J17497–2821 is in a typical LHS in which unsaturated Comptonization is believed to be the main physical process at work. In this regime, a 150 keV cut-off leads to an estimated corona temperature of about 75 keV. Seed photons and Comptonizing plasma are far from being in thermal equilibrium and a large fraction of energy is exchanged at each interaction. In these conditions, models such as COMPPS (Poutanen & Svensson 1996) that uses iterative scattering numerical procedures is more suitable than e.g. COMPTT. Indeed the latter model is basically valid in the diffusion regime, i.e. when the *average* photon energy exchange per scattering is small ($\Delta E/E \ll 1$) and photons suffer many scatterings when traveling across the plasma before escaping (see Farinelli et al, 2008, for a discussion on Comptonization models).

[5] R_{in}^{seed} was not corrected for the inclination since the Comptonized emission is more likely isotropic.

Our detection of the source up to 300 keV strengthens the interpretation of an X-ray Nova: Comptonization is believed to be the dominating process at work in these objects and a signal up to 300 keV implies very high plasma temperatures that are more common in BHs in their LHS. Indeed, unlike for BHs, in the case of a NS the surface is an additional source of seed photons that controls the plasma temperature through Compton cooling (Barret 2001).

4.2. X-ray Novae: far from canonical

Novae are known to show a series of different X-ray spectral states during their outburst. The "canonical" evolution, i.e. the first one seen in X-ray transients, shows a spectral softening while the flux increases and then a hardening during decay, towards quiescence. The advent of many X-ray missions together with their monitoring capabilities has proven that this standard evolution is far from being the only one. A certain number of X-ray Novae has shown outbursts with a single spectral state, the Low Hard State with $\Gamma < 2$ all along the outburst (e.g. Rodriguez et al., 2006, and references therein). This is also the case for IGR J17497–2821 that remained hard during the outburst, with a possible hardening along the decay. It has further been assumed that "canonical" X-ray transients follow the Fast Rise Exponential Decay morphology whereas this is frequently not the case; even in the genuinely soft sources a precursor low/hard state phase is seen prior to the fast rise in all cases where data are available (Brocksopp et al. 2002). Furthermore, a correlation between luminosity and spectral softness is not necessarily observed in all sources (Brocksopp et al. 2004) and evidence for a spectral softening in the last phases of the decay while entering in quiescence has also been found (Tomsick et al. 2004).

5. Conclusions

We have presented the best broad-band high energy spectrum currently available for the X-ray transient IGR J17497–2821. A fit with a simple phenomenological model gave a constrained high energy cut-off around 150 keV, naturally driving the choice for the model used to interpret the data in a physical scenario. Soft seed photons coming from the disc are thermally up-scattered by a hot and patchy corona. A very mild reflection component is seen for the first time in the spectrum. Though not conclusive, there is a hint of spectral hardening about 10 days after the peak outburst with the source remaining in its LHS all along the outburst.
Explaining within a self consistent scenario a "canonical" BH LMXB (e.g. XTE J1550–564 Rodriguez et al. 2003), the LHS outburst of e.g. IGR J17497–2821 (this work) and the final softening towards quiescence (e.g. XTE J1650–500 Tomsick et al. 2004) is a real challenge, essential to really understand the physics of accretion. Broad-band studies are the first important step to have a complete view of the source spectral properties in the X-ray domain, where the accretion power resides.

This work has been supported by the Japan Society for the Promotion of Science (JSPS) grant in the frame of the short-term Postdoctoral Fellowship for Foreign Researchers (March-April 2008). AP thanks JAXA/ISAS, where most of the work has been done, for their kind hospitality and interesting scientific (and cultural!) discussions. AP acknowledges the Italian Space Agency financial and programmatic support via contract I/008/07/0.

References

Barret, D. 2001, Advances in Space Research, 28, 307
Brocksopp, C et al., 2004, NewA 9, 249
Brocksopp, C et al., 2002, MNRAS 331, 765
Dickey, J. M., & Lockman, F. J. 1990, ARA&A, 28, 215
George, I. M., & Fabian, A. C. 1991, MNRAS, 249, 352
Itoh, T., et al. 2006, The Astronomer's Telegram, 914, 1
Farinelli et al. 2008, ApJ 680, 602
Fukazawa et al., 2008, JX-ISAS-SUZAKU-MEMO-2008-01, "Reproducibility of the HXD-GSO Non X-ray Background for the ver 2.0 processing data", http://www.astro.isas.jaxa.jp/suzaku/doc/suzakumemo/
Gierlinski, M. et al. 1997, MNRAS, 288, 958
Kennea, J. A. et al. 2006, Astronomer's Telegram, 900, 1
Kokubun, M. et al. 2007, PASJ, 59, S53
Koyama, K., et al. 2007, PASJ, 59, S23
Makishima, K., et al. 2008, ArXiv e-prints, 801, arXiv:0801.3315
Makishima, K., et al. 2000, ApJ, 535, 632
Mitsuda, K., et al. 2007, PASJ, 59, S1
Mitsuda, K. et al. 1984, PASJ 36, 741
Morrison, R and McCammon, D, 1983 ApJ 270, 119
Paizis, A., et al. 2007, ApJL, 657, L109
Poutanen, J. & Svensson, R. 1996, ApJ, 470, 249
Rodriguez, J., et al. 2007, ApJL, 655, L97
Rodriguez, J., Shaw, S. E., & Corbel, S. 2006, A&A, 451, 1045
Rodriguez, J., Corbel, S., & Tomsick, J. A. 2003, ApJ, 595, 1032
Serlemitsos, P. et al., 2007, PASJ, 59, S9
Soldi, S., et al. 2006, The Astronomer's Telegram, 885, 1
Takahashi, H., et al. 2008, PASJ, 60, 69
Takahashi, T. et al. 2007, PASJ, 59, S35
Titarchuk, L., 1994 ApJ 434, 570
Titarchuk, L., & Shaposhnikov, N. 2005, ApJ, 626, 298
Tomsick et al. 2004, ApJ 601, 439
Torres, M. A. P. et al. 2007, The Astronomer's Telegram, 1002, 1
Torres, M. A. P. et al. 2006, The Astronomer's Telegram, 909, 1
Walter, R., et al. 2007, A&A, 461, L17
Winkler, C., et al. 2003, A&A, 411, L1